Machine Vision and Applications (1988) 1:155–162

Machine Vision and Applications


# Background Subtraction Algorithms for Videodensitometric Quantification of Coronary Stenosis

O. Nalcioglu*,**, W.W. Roeck*, T. Reese*, L.Z. Qu*, J.M. Tobis**, and W.L. Henry**

*Department of Radiological Sciences Division of Physics and Engineering and **Department of Medicine (Cardiology) University of California, Irvine

**Abstract:** The determination of percent stenosis of coronary arteries is an important task in medicine. In this paper we discuss three different algorithms which can be used in conjunction with videodensitometry to measure this quantity. These algorithms may be used in subtracting the background under a vessel segment thus eliminating the need for a preinjection mask. Mathematical details of the algorithms and experimental results are presented.

**Key Words:** stenosis, videodensitometry, digital radiography, background subtraction

## 1. Introduction

Recent advances in the digital x-ray video imaging systems have made the visualization and measurement of small amounts of radiopaque contrast agents within the vasculature a reality. The components of a typical digital radiographic system are the x-ray generator, x-ray tube, intensifier (II), television (TV) camera, video digitizer, display, and recording devices. Two general classes of measurements one can perform using the digital video images are: (a) geometrical (Selzer 1976) and (b) videodensitometric quantification (Sandor 1979; Spears et al. 1980; Reiber et al. 1983; Roeck et al. 1981; Nichols et al. 1985). Here, we will only be concerned with the latter. Videodensitometric measurements (Baily 1980) are based on the linear relationship between the intensity of the video signal and the thickness of the tissue transversed by x-rays causing that signal. Many physical problems, some of which are intrinsic to such imaging systems and others which are due to the nature of interaction of x-rays with an object, usually cause a deviation from this desired linear relationship (Nalcioglu 1986). Thus, it is quite essential to determine the response of the imaging chain prior to making measurements on images obtained with such systems. In this paper, we will focus on the videodensitometric measurement of coronary stenosis. The most common technique used for this purpose is the "mask subtraction" (Mistretta et al. 1978). In this technique, a mask image of the patient is taken prior to the injection of iodinated contrast material into the coronary vessels. Then, a pixel-by-pixel subtraction of the logarithmically amplified mask image from the post-injection image results in an image which "ideally" has all the noniodinated parts of the object cancelled. The net iodine signal intensity is linearly related to the thickness of the vessel containing it. Thus, a correct measurement requires, among other things, a total cancellation of the noniodinated overlaying structures. If the patient moves in between the time the mask and post-injection images are acquired, then the difference images may be degraded due to motion artifacts. The measurement of coronary stenosis using such images would give rise to different degrees of error depending on the magnitude and location of motion artifacts. Since the physiological motions which occur in a patient are not simple translational motion, one can not remedy the situation by simply shifting the mask to obtain an acceptable registration with the iodinated image. Attempts to alleviate this problem by means of rubber sheet algorithms have proven to be difficult and at best, approximate. In

*Address reprint requests to:* Dr. Orhan Nalcioglu, Dept. of Radiological Sciences, B 135 Med. Sci. 1, California College of Medicine, University of California, Irvine, CA 92717 USA.

This work was supported in part by PHS Grant No. HL31440, awarded by the National Heart, Lung, and Blood Institute, DHHS. The authors also acknowledge a research grant awarded by Philips Medical Systems, Inc.

this paper, we discuss several different algorithms to estimate the background under the iodinated vessel. Since the background is derived from the iodinated images, one does not have to use any pre-injection mask images. Section 2 covers the theory. The results are presented in Section 3 and the conclusions are given in Section 4.

## 2. Theory

### 2.1 Basic Formalism

The expression for a two-dimensional video image $U(x,y)$ obtained with a TV based x-ray imaging system is given by Kruger (1978) as

$$U(x,y) = a[I(x,y)]\gamma \quad (1)$$

where $a$ is an amplification factor and $\gamma$ a constant. It should be emphasized that for a dynamic system such as the cardiovascular system, images are also an explicit function of time. In this paper the time dependence will be kept implicit. The function $I$ is related to the transmitted photon fluence by

$$I(x,y) = \alpha\, N(x,y) \quad (2)$$

where $\alpha$ is an amplification constant and $N$ is defined by

$$N(x,y) = P(x,y) + S(x,y) \quad (3)$$

In Eq. (3), $P$ and $S$ are the primary and scattered x-ray distribution components, respectively. The primary x-ray component $P$ is related to the incident one by the following equation.

$$P(x,y) = N_o(x,y) \exp\left[-\int \mu\,(x,y,z: <E>)\, dz\right] \quad (4)$$

where $N_o$ is the incident x-ray flux at location $(x,y)$ and $\mu$ the spatially position-dependent linear attenuation coefficient along the x-ray beam direction which was assumed to be along the z axis. Note that in writing Eq. (4), we ignored the polychromaticity of the x-ray beam. The approximation of taking the attenuation coefficient at an effective energy $<E>$ appears to be a good approximation when one attempts to determine coronary stenosis by videodensitometry. The scatter component $S$ is related to the incident flux by a complex relationship. In most physical situations, the scatter component $S$ does not contain any high spatial frequencies, that is, it is a slowly varying function of spatial coordinates (x,y) over the dimensions of the vessel. In Eqs. (2) to (4) we also assumed that other physical problems such as veiling glare which are inherent to image intensifier based systems are not significant for the measurement of coronary stenosis even though they cause an overall reduction in image contrast.

Since the measurement of coronary stenosis involves the injection of iodine into the vessels, we will now deal with this situation. The primary signal after the contrast material is injected into the vessels is given by

$$P_I(x,y) = P(x,y) \exp\left[-\int \mu_I(x,y,z: <E>)\, dz\right] \quad (5)$$

where $\mu_I$ is the iodine linear attenuation coefficient measured with respect to blood which was displaced by the contrast agent. From now on, we will implicitly assume that the spatial extent of (x,y) in all the equations is limited to within the boundaries of the vessel where a videodensitometric measurement is to be performed. Using the new primary signal $P_I$ in Eq. (3) and taking the logarithm of the video signal $U_I$ results in

$$\ln U_I(x,y) \approx \delta\,\{\ln[N(x,y)] - \int \mu_I (x,y,z: <E>)\, dz\, [P(x,y)/N(x,y)]\} \quad (6)$$

where $\delta$ is a constant and $N$ defined by Eq. (3) is the background signal under the iodinated vessel. In writing Eq. (6), it was also assumed that the signal from the iodinated vessel is much smaller than the background signal under it. We will now rewrite Eq. (6) as

$$\ln U_I(x,y) = \delta \ln N(x,y) - \beta \int \mu_I\,(x,y,z: <E>)\, dz \quad (7)$$

where we defined $\beta = \delta P(x,y)/N(x,y)$. The constant $\beta$ is independent of (x,y) in a first order approximation. The last term in Eq. (7) can further be simplified by assuming that the contrast material is homogeneously mixed within the vessel. This results in

$$\Gamma\,(x,y) = \beta\, \mu_I(<E>) \int dz \quad (8)$$

where we moved the attenuation coefficient $\mu_I$ outside the integral sign. It should be pointed out that in Eq. (8), the integral over z is equal to the thickness of vessels $L(x,y)$ in the direction of the x-ray beam at a location (x,y). The first term in Eq. (7) results from the background under the vessel. A videodensitometric determination of vessel volume requires the subtraction of the background term from Eq. (7) and integration of the resultant signal over (x,y) within the boundaries of the vessel segment under consideration. In the mask subtraction technique, the background term in Eq. (7) is eliminated by choosing an image of the region of interest prior to the arrival of iodine. However, since the

mask and postinjection images are obtained at different times, there is a great probability that they may not be in perfect registration even if one uses ECG gating.

Let us assume that we have a vessel segment where we wish to measure the cross section videodensitometrically; the situation is illustrated in Figure 1. The cross section to be determined is perpendicular to the length of the vessel which was taken to be in the direction of A–D. If the cross section of the vessel does not change appreciably along its length, it proves to be advantageous to measure the vessel volume bounded by A′B′C′D′ and dividing it by the height $h$ to obtain an average cross-sectional area. The height $h$ should be chosen such that the vessel cross section does not vary significantly within this distance. It should be emphasized that the location of points A′B′C′D′ need not be at the edges of the vessel. This actually proves to be one of the main advantages of the videodensitometric techniques over the edge detection schemes. In practice, these points are chosen to be as close to the visualized edges as possible but intentionally placed outside the vessel boundaries. The reason for close proximity is due to the fact that we wish the segments AA′ and B′B to represent the background area (see Figure 2). Positioning these points at the vessel edges might provide a more accurate representation of background regions, but then one has to worry about the inaccuracies introduced by the edge detection technique employed, especially in the presence of noise. It is our experience that if these points are chosen to be several pixels away

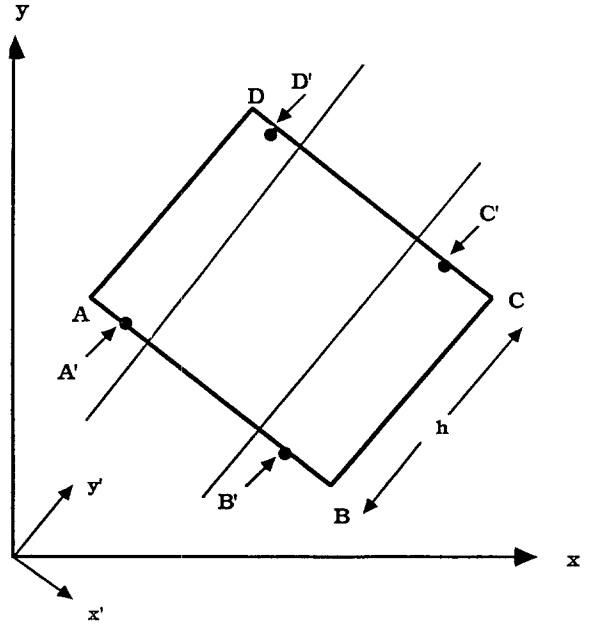


Figure 1. Selection of a region of interest (ROI).

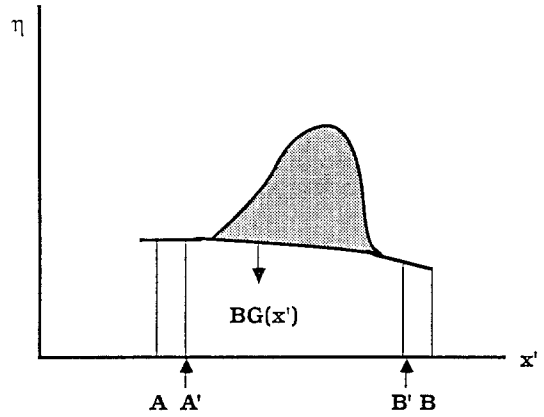


Figure 2. Integrated videodensity profile η as a function of distance X′ perpendicular to the vessel edges. The vessel edges (cf. Fig. 1) are marked by A′B′. The net video signal proportional to the vessel volume is indicated by shaded area. The interpolated background is denoted by $BG(x')$ bounded by ABCD along a vessel bounded by A′B′C′D′. The length of the vessel is marked by $h$.

from the edges, one usually obtains a fairly accurate background estimation by using the algorithms discussed in this paper. The logarithmically amplified video signal from Eq. (7) can be integrated along the y′ direction to obtain

$$\eta(x') \equiv -\int \ln U_I(x',y')\,dy' = -\delta \int \ln N(x',y')\,dy' + \beta\,\mu_I(\langle E\rangle) \int L(x',y')\,dy' \tag{9}$$

The function η which is defined in Eq. (9) is illustrated in Figure 2. In order to calculate the net video signal from the iodine filled vessel (shaded area), we have to subtract the background area within $A' \leqslant x' \leqslant B'$. Let us denote the background signal along the x′ direction by $BG(x')$. This corresponds to the first term on the right hand side of Eq. (9). The computation of the cross sectional area is achieved by evaluating

$$\int_{A'}^{B'} [\eta(x') - BG(x')]\,dx' = \beta\mu_I(\langle E\rangle) \iint L(x',y')dx'dy' \tag{10}$$

The double integral term in Eq. (10) is the volume of the vessel bounded within the area A′B′C′D′. Dividing Eq. (10) by the length of the vessel $h$ yields

$$\Delta \equiv \int_{A'}^{B'} [\eta(x') - BG(x')]dx'/h = \beta\mu_I(\langle E\rangle)\,\langle A\rangle \tag{11}$$

where $\langle A\rangle$ is the average cross-sectional area of the vessel along the segment under consideration.

The percent area stenosis is computed by

$$S_A = 100\,[1 - \Delta_s/\Delta_p] \tag{12}$$

where $\Delta_s$ and $\Delta_p$ are related to the cross-sectional areas of the stenotic and patent vessels, respectively [cf. Eq. (11)]. In the following sections, we will introduce various algorithms for the estimation of background $BG(x')$ under the vessel, that is, for $A' \leq x' \leq B'$. If the vessel cross section varies rapidly along the vessel, that is, along A–D in Figure 1, one may have to use a two-dimensional interpolation scheme. Such techniques have been discussed by Douglass et al. (1981) and Nalcioglu et al. (1983).

### 2.2 Background Interpolation Algorithms

The problem to be solved is the estimation of the background $BG(x')$ within $A' \leq x' \leq B'$ from a knowledge of its values for $x' < A'$ and $x' > B'$; see Figure 2.

**2.2.1 Linear interpolation (LIN) method.** In this subsection we will assume the background to be linear under the vessel, that is, for $A' \leq x' \leq B'$. The background is estimated by computing its average values from two adjacent regions outside the vessel. These regions will be taken to be:

$$A \leq x' \leq A' \tag{13.a}$$
$$B' \leq x' \leq B \tag{13.b}$$

The average values are given by

$$BGL = \int_A^{A'} BG(x')\,dx'/(A' - A) \tag{14.a}$$
$$BGR = \int_{B'}^{B} BG(x')\,dx'/(B - B') \tag{14.b}$$

The estimated background $BGE_1$ is defined by

$$BGE_1(x') = mx' + n \tag{15}$$

where

$$m = 2[BGR - BGL]/[B + B' - A - A'] \tag{16.a}$$
$$n = [(B + B')\,BGL - (A + A')BGR]/[B + B' - A - A'] \tag{16.b}$$

The videodensitometric cross-sectional area is computed by

$$\Delta_1 = \int_{A'}^{B'} [\eta(x') - BGE_1(x')]\,dx'/h \tag{17}$$

which is similar to Eq. (11).

**2.2.2 Least mean squared error (LMSE) method.** Let us assume that the background can be approximated as a polynomial given by

$$BGE_2(x') = \sum_{k=0}^{M} a_k\,(x')^k \tag{18}$$

The mean error between the actual background $BG(x')$ and the estimated one is minimized by computing

$$(\partial\,\epsilon/\partial\,a_k) = 0 \tag{19}$$

where

$$\epsilon = \sum_{j=1}^{N} [BG(x'_j) - BGE_2(x'_j)]^2 \tag{20}$$

In Eq. (20) the summation over $j$ is performed for values of $x'$ given in Eq. (13), that is, regions adjacent to but outside the vessel boundaries. Computation of the coefficients $a_k$ is achieved by using Eqs. (18–20) and using a matrix inversion to obtain $a_k$. The net iodine signal is given by

$$\Delta_2 = \int_{A'}^{B'} [\eta(x') - BGE_2(x')]\,dx'/h \tag{21}$$

**2.2.3 Cubic spline interpolation (CSI) method.** The procedure can be explained with the aid of Figure 2. First, we perform a separate mean least squares fit to the background in the two regions using:

$$b_L(x') = \sum_{k=0}^{M_L} a_k(x')^k \quad A \leq x' \leq A' \tag{22.a}$$
$$b_R(x') = \sum_{k=0}^{M_R} c_k(x')^k \quad B' \leq x' \leq B \tag{22.b}$$

Once we determine $a_k$ and $c_k$ according to the procedure given in Subsection 2.2.2, we then know both of these background functions. The cubic spline process involves fitting a third order polynomial $BGE_3(x')$ within $A' \leq x' \leq B'$ in such a way that the following conditions hold:

$$BGE_3(x'_{A'}) = b_L(x'_{A'}) \quad (23.a)$$

$$d(BGE_3)/dx' = d(b_L)/dx' \text{ at } x' = x'_{A'} \quad (23.b)$$

$$BGE_3(x'_{B'}) = b_R(x'_{B'}) \quad (23.c)$$

$$d(BGE_3)/dx' = d(b_R)/dx' \text{ at } x' = x'_{B'} \quad (23.d)$$

If the cubic polynomial is given by

$$BGE_3(x') = A_0 + A_1(x') + A_2(x')^2 + A_3(x')^3 \quad (24)$$

we can determine $A_i$ for $0 \leq i \leq 3$ using the conditions given in Eq. (23) since we already know $b_L$ and $b_R$ from Eq. (22). The net iodine signal is determined by $\Delta_3$ evaluated as

$$\Delta_3 = \int_{A'}^{B'} [\eta(x') - BGE_3(x')]\, dx'/h \quad (25)$$

## 3. Results

### 3.1 System Linearity

In order to test the linearity of the system in measuring volumes, we performed a series of experiments using five balloons filled with 7, 14, 21, 31 and 41 cc of 10% Renografin-76 and placed inside a chest phantom one at a time. A mask image of the chest phantom without any balloons was also acquired under the same experimental conditions. The concentration of iodine used in these experiments corresponds to 37 mg iodine/cc which is less than what is commonly used in coronary angiography but similar to intraveneous angiography. The images were obtained at 70 kVp and 50 mAs with 4 mm added aluminum filtration. An x-ray grid was placed on the image intensifier to reduce the effects of x-ray scatter. The images were digitized into 512 × 512 format with 8 bits per pixel. All six images were logarithmically amplified pixel by pixel prior to data analysis. The "mask" image which did not contain any balloons was subtracted pixel by pixel from five other images containing the balloons with different volumes of the iodine mixture. The resultant signal in the subtracted images is given by Eq. (8) which states that the intensity at a given location (x,y) is proportional to the thickness of object traversed by x-rays. The constant of proportionality in Eq. (8) is given by $\beta\, \mu_I$ where $\mu_I$ is the effective linear attenuation coefficient of the iodine mixture. If one integrates Eq. (8) over x and y within a region of interest (ROI) encompassing the projection of the object, one obtains

$$Q = \beta\, \mu_I (\langle E \rangle) \iint dx\, dy \int dz(x,y) \quad (26)$$

In Eq. (26) the two-dimensional integral over (x,y) is performed within the ROI and one does not have to know the exact location of the edges of the object as long as the ROI completely covers the object's projection within the subtracted image. If the ROI is larger than the object's projection the points outside the object contribute nothing since they are eliminated by mask subtraction. We have introduced the explicit (x,y) dependence into z in Eq. (26), since the thickness of the object depends on the location (x,y). Equation (26) can also be rewritten as

$$Q = \delta V \quad (27)$$

where $V$ is the absolute volume of the iodine filled balloon and $\delta = \beta\, \mu_I$ is the constant of proportionality. Thus, for relative volume measurements such as percentage stenosis, one does not have to know $\delta$ as long as it is constant within the object, that is, homogeneous mixing of iodine. It should be pointed out that the value of $Q$ or $V$ is independent of the shape of the object. This actually is the beauty of videodensitometric technique which does not have to make any assumptions regarding the shape of the volume filled with the contrast medium. Of course, if one is interested in determining the absolute volume $V$, the constant of proportionality $\delta$ has to be determined by some other means. It should also be emphasized that any heterogeneous mixing of iodine would cause measurement errors depending on the degree of imperfect mixing. The linearity results obtained by changing the balloon volume are shown in Figure 3. The vertical axis indicates the video-

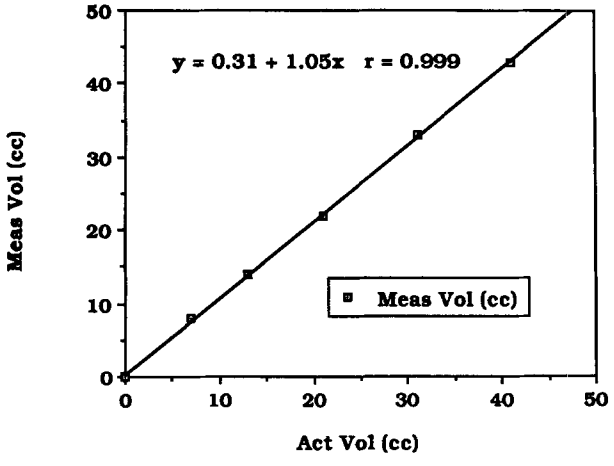


Figure 3. Videodensitometrically measured balloon volume (vertical axis) vs. actual balloon volume (horizontal axis), all in cc's. The best fit line is also shown.

densitometrically measured volume in cc's. The actual volumes are given along the horizontal axis. The conversion of relative volumes into absolute ones was done by: (a) fitting a straight line through the experimentally measured relative volumes using a linear least squares fit and then (b) normalizing the slope of the straight line which is given as $\delta$ in Eq. (27) at the last measurement point. The first point results from subtracting the mask image from itself resulting in $V = 0$. The linearity of data in Figure 3 indicating the capability of the system in measuring relative volumes is quite impressive.

### 3.2 Phantom Studies

In these studies, a phantom consisting of a Plexiglas block containing holes was used. An illustration of the phantom is seen in Figure 4. The diameter of the patent segment was 4 mm. The diameter of the stenotic segment was 0.51, 0.71, 0.99, 1.51 and 1.99 (all in mm) in five different blocks. The holes were filled with 50% Cysto-Conray II (81 mg/ml organically bound iodine). The x-ray tube was operated at 75 kVp with a 4 mm aluminum added filter. In the first case, five Plexiglas blocks were placed behind 10 cm thickness of plexiglas to provide a uniform background. A second study was performed in which the same blocks were placed within a chest phantom one by one to simulate a more realistic nonuniform background. Figure 5 shows an x-ray image of the chest phantom with a Plexiglas block filled with Cysto-Conray II in place. The x-ray images were digitized into 512 × 512 format using an 8-bit analog-to-digital converter (ADC) and stored in a video RAM for image analysis.

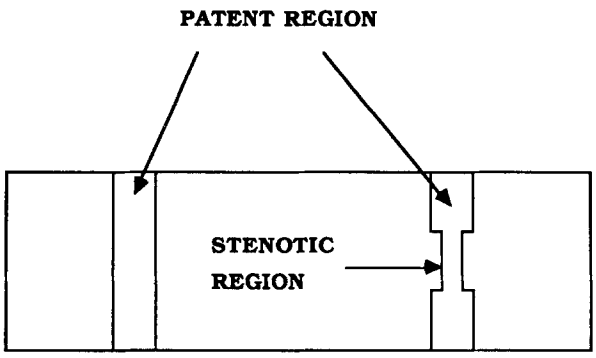


Figure 4. An illustration of the plexiglas block phantom.

Figure 5. An x-ray image of the chest phantom with the stenosis phantom in place.

#### 3.2.1 Linear background interpolation (LIN).

Five images with the uniform background were analyzed using the linear background interpolation algorithm given in Subsection 2.2.1. A similar calculation was repeated on the second set of five images which included the chest phantom as the background. The net video signal was computed using Eq. (17) for the patent and stenotic regions for all images. The percent area stenosis was calculated using Eq. (12). Figure 6 summarizes the results of such a calculation. The density profiles corresponding to two regions are displayed at the bottom of the figure. The results comparing the actual and video-densitometrically measured percent area stenosis are plotted in Figure 7. The straight lines shown in the figure were obtained by a linear least squares fit. The data displayed by open squares was obtained

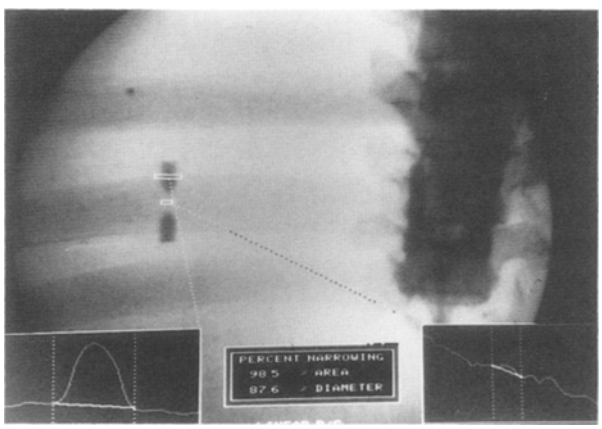

Figure 6. An example of the linear background interpolation method for the measurement of percent stenosis with the chest phantom.

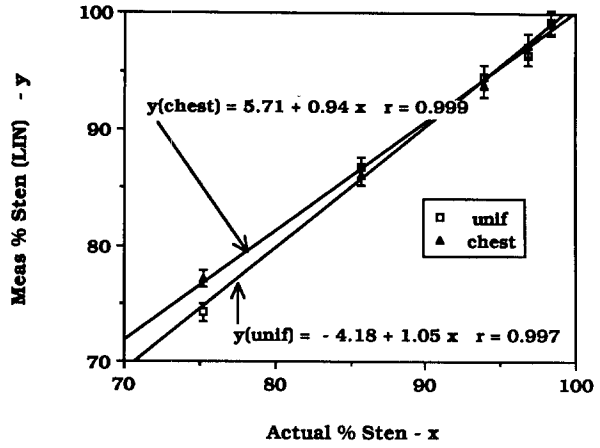


Figure 7. Videodensitometrically measured percent stenosis for the two phantoms vs. the actual values, using the LIN method. Unif; uniform background, Chest; chest phantom.

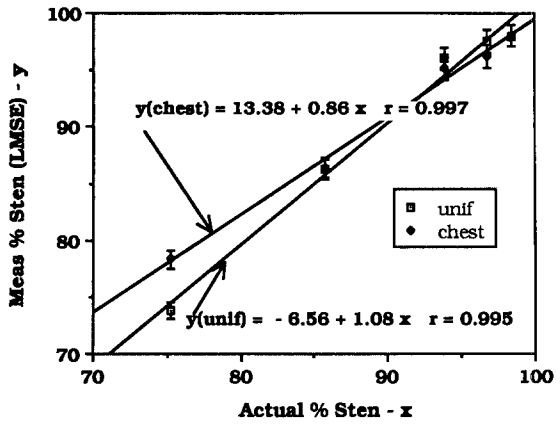


Figure 9. Videodensitometrically measured percent stenosis for the two phantoms vs. the actual values using the LMSE method. Unif; uniform background, Chest; chest phantom.

with the uniform background phantom. The data arising from the chest phantom is shown with solid triangles. We observe that with the linear background interpolation method (LIN) the videodensitometric measurement of percent stenosis for both phantoms correlates well with the actual values.

**3.2.2 Least mean squared error (LMSE) method.** The LMSE algorithm described in Subsection 2.2.2 was used in analyzing the same images as in the previous subsection. The order of the polynomial in Eq. (18) was taken to be 4. Figure 8 summarizes the results of the LMSE method. The density profiles corresponding to the stenotic and patent regions are displayed at the bottom. The graphs of the measured videodensitometric percent stenosis for the two sets of images are shown in Figure 9. The correlation of the videodensitometric data with the actual percent stenosis measurements seems quite satisfactory.

**3.2.3 Cubic spline interpolation (CSI).** In this case, we applied the CSI algorithm described in Subsection 2.2.3 to compute the percent stenosis using the same images as discussed before. A typical result is shown in Figure 10. The density profiles given in the figure correspond to the patent and stenotic regions. A plot of videodensitometric CSI measurements versus the actual ones is shown in Figure 11. The correlation of measured data with the actual ones again is quite good.

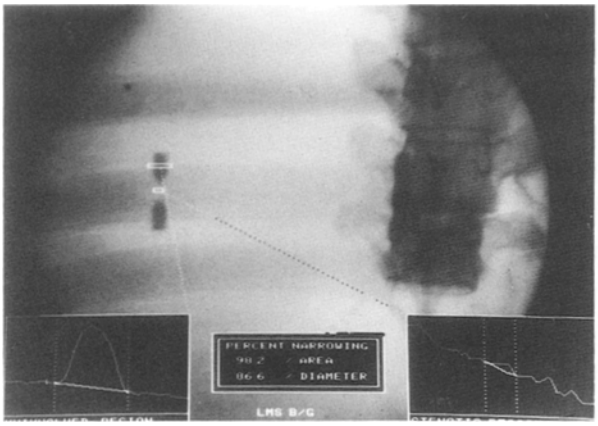


Figure 8. An example of the LMSE method for the measurement of percent stenosis with the chest phantom.


Figure 10. An example of the CSI method for the measurement of percent stenosis with the chest phantom.

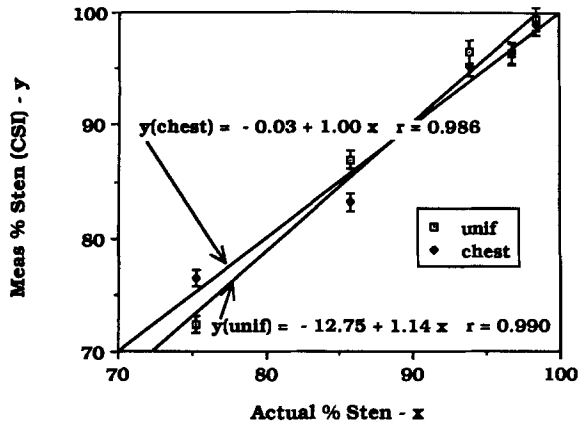


Figure 11. Videodensitometrically measured percent stenosis for the two phantoms vs. the actual values using the CSI method. Unif; uniform background, Chest; chest phantom.

## 4. Conclusions

We have shown that videodensitometric determination of percent area stenosis can be acheived accurately by using three different background subtraction algorithms. The experimental results presented in this paper indicate that all three algorithms provide highly accurate determination of percent area stenosis. Even though the data presented in this paper indicates that all three algorithms perform equally well for the two phantoms used in these experiments, it is obvious that when the background under the vessel is not linear within the dimension of the vessel, the linear background subtraction method will be inferior to the LMSE or CSI techniques. The performance of each algorithm is also dependent upon the actual situation at hand. The reason there is no significant difference in the performance of any of the three techniques is possibly due to the phantoms used in this study. We have also seen from the presented results that the physical problems such as veiling glare, beam hardening, and x-ray scatter do not affect the measurement of percent stenosis. All the computations presented here can be performed quite rapidly in a video image processor. The main advantage of the three techniques discussed in this paper is that one does not have to perform subtraction of any mask obtained prior to contrast material injection, thus avoiding any possible misregistration artifacts.

## References

Baily NA (1980) Video techniques for x-ray imaging and data extraction from roentgenographic and fluoroscopic presentations. Med. Phys. 7, 472–491

Douglass KH, Links JM, Gedra T, Wagner HN (1981) A comparison of interpolative background subtraction algorithms using analytical surfaces. In: Esser (ed) Functional mapping of organ systems. The Society of Nuclear Medicine, pp 83–101

Kruger RA (1978) Time dependent subtraction imaging. Ph.D. thesis, University of Wisconsin

Mistretta CA, Kruger RA, Houk TL, Riederer SJ, Shaw CG, Ergun D, Kubal W, Crummy AB, Ziebel W, Rowe G, Zarnstorff W, Flemming D (1978) Computerized fluoroscopic techniques for non-invasive cardiovascular imaging. Proc. SPIE 152, 65–71

Nalcioglu O, Lando AV, Boone JM, Roeck WW, Tobis JM, Henry WL (1983) Quantification of coronary stenoses from digital images. Circ. 68, Supp. III, 346

Nalcioglu O, Roeck WW, Seibert A, Lando AV (1986) Quantitative aspects of digital fluoroscopy. In: Thomas and Kereiakes (eds) Digital radiography. Plenum Publishing Co., New York, pp 83–132

Nichols AB, Han J, Esser DP (1985) Cinevideodensitometric analysis of flow-limiting coronary stenotic lesions. Circ. 72, Supp. III, 388

Reiber JHC, Slager CJ, Schuurbiers JCH, den Boer A, Gerbrands JJ, Troost GJ, Schotts B, Kooijman CJ, Serruys PW (1983) Transfer functions of the x-ray-cine-video chain applied to digital processing of coronary cineangiograms. In: Heintzen and Brennecke (eds) Digital imaging in cardiovascular radiology. Georg Thieme Verlag, Stuttgart, pp 89–104

Roeck WW, Nalcioglu O, Seibert JA (1981) Hybrid system for high resolution videodensitometry. Proc. SPIE 314, 92–100

Sandor T, Als AV, Paulin S (1979) Cine-densitometric measurement of coronary arterial stenoses. Cath. and Cardiovasc. Diagn. 5, 229–245

Selzer RH, Blankenhorn DH, Crawford DW, Brook SH, Barndt R (1976) Computer analysis of cardiovascular imagery. Proc. CALTEC/JPL Conf. Image Proc. Tech. pp 6-1 to 6-20

Spears JR (1981) Rotating step-wedge technique for extraction of luminar cross-sectional area information from coronary cineangiograms. Acta Radiol. Diag. 22, 217–225